CFD modelling of atrium-assisted natural ventilation

Ji, Y, Cook, M and Hunt, G

CFD Modelling of Atrium-assisted Natural Ventilation

Y. Ji[1], M. J. Cook[1] and G. R. Hunt[2]

[1]Institute of Energy and Sustainable Development, De Montfort University,
The Gateway, Leicester, LE1 9BH, UK
Email: yingchun@dmu.ac.uk http://www.iesd.dmu.ac.uk/
[2]Department of Civil and Environmental Engineering, Imperial College London, London, SW7 2BU, UK

Summary: *Using computational fluid dynamics (CFD) techniques to model buoyancy-driven airflows has always proved challenging. This work investigates CFD modelling of buoyancy-driven natural ventilation flows in a single-storey space connected to an atrium. The atrium is taller than the ventilated space and when warmed by internal heat gains producing a column of warm air in the atrium and connect space drives a ventilation flow. Results of CFD simulations are compared with predictions of an analytical model and small-scale experiments [1]. Using the RNG k-epsilon turbulence model the predicted airflow patterns and temperature profile agreed reasonably well between the three prediction techniques. The work demonstrates the potential of using CFD for modelling natural displacement ventilation and the accuracy that can be expected.*

Keywords: *CFD, atrium, RNG k-epsilon turbulence model, natural ventilation, buoyancy*
Category: *Natural Ventilation*

1 Introduction

Over recent years natural ventilation has become more common in modern building design as an energy efficient means of providing fresh air for occupants in large non-domestic buildings. Natural driving pressures created by warm air inside buildings can be used to drive a flow through a room by means of the stack effect. In order to enhance the ventilation rates, an adjoining atrium extending above the ventilated space can be used which increases the natural driving force by increasing the depth of the warm air column. To gain a deeper understanding of this ventilation strategy, the main features of the flow (Figure 1) have been studied using simplified mathematical models and small-scale laboratory experiments [1].

An ability to model natural ventilation at the design stage is important for understanding the flow characteristics, including likely ventilation rates, temperature stratification and fresh air distribution. Techniques for predicting these parameters include analytical methods, experimental techniques and computational fluid dynamics (CFD). CFD has the advantage over analytical and experimental methods of providing air speed and temperature data at many locations throughout the flow field. However, difficulties have long been reported [2] when modelling pure natural convection in buildings using CFD due to the weak coupling between the enthalpy and momentum equations and a lack of knowledge on the boundary conditions at openings. Although some work has been done to address these difficulties [3], further validation is needed before applying this numerical method as an independent tool to natural ventilation design with confidence. Cook & Lomas [3] showed comparisons between physical and CFD modelling of natural convection flow for a single space with a localised heat source and openings connected to external air. An external fluid domain was used for this work in order to avoid inaccuracies in specifying boundary conditions directly at the ventilation openings; the technique was successful despite an increase in computation time.

This paper describes a benchmark test case used for evaluating the ability of CFD for modelling buoyancy-driven displacement ventilation of a space connected to an atrium. The benchmark is validated using analytical and experimental work carried out by Holford & Hunt [1] which is described in section 2. Section 3 describes the CFD modelling techniques adopted and the results and conclusions are given in section 4 and 5 respectively.

2 Mathematical models and experiments

Figure 1 shows a natural ventilation system in which a single space is connected to a tall atrium. The airflow path includes a Top-Down-Chimney (TDC) inlet, a TDC, a storey inlet, a storey outlet and an atrium outlet, these are denoted by the labels 1 to 5 in figure 1 with cross-sectional areas a_1 to a_5 and corresponding loss coefficients C_{d1} to C_{d5} respectively. A general expression for the effective opening area A_n for a particular part of the flow path can be expressed as:

$$\frac{1}{A_n^2} = \sum_{i=m}^{n} \left(\frac{1}{2C_{di}^2 a_i^2} \right) \qquad (1)$$

where $1 \le m \le n \le 5$.

Mathematical expressions for predicting the volume flux Q and the reduced gravity G' in a plume generated by a localised point heat source with strength B (m^4s^{-3}) as a function of the distance x from the source were given by [4]. Assuming zero initial momentum and volume flux, Q and G' are given by:

$$Q(x,B) = C(Bx^5)^{1/3} \quad (2)$$

$$G'(x,B) = (B^2x^{-5})^{1/3} / C \quad (3)$$

where C is a constant, ≈ 0.14.

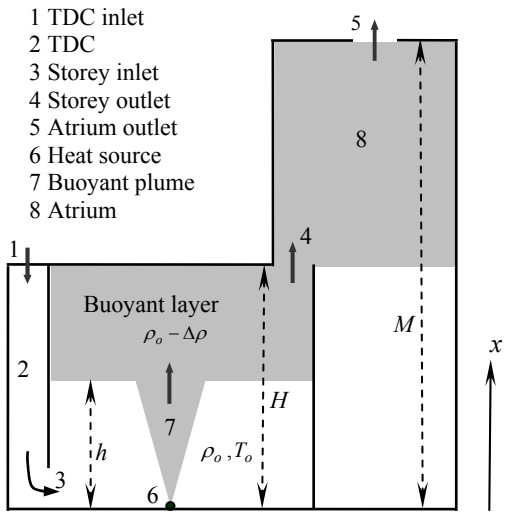

Figure 1. Natural ventilation of a space connected to an atrium following [1].

In the absence of the atrium and top-down chimney (Figure 1) Linden et al [5] derived the following expression for the single ventilated space:

$$\frac{A_s}{H^2} = \sqrt{C^3\xi^5/(1-\xi)} \quad (4)$$

where ξ $(= h/H)$ is the dimensionless interface height and A_s is the effective opening area of the storey (with $m = 1$ and $n = 4$ in equation (1)).

Denoting ρ_o and T_o as the density and temperature of the ambient air, and $\Delta\rho$ and ΔT the density and temperature differences between the ambient and the warm upper layer, the reduced gravity g' is given by $g' = g\Delta\rho/\rho_o = -g\Delta T/T_o = G'(x = h, B)$ and $\rho_o g'(H-h)$ is the stack pressure driving the flow. When the space is connected to a tall atrium of height M, the steady depth of the warm buoyant layer is increased to $(M-h)$, and the driving pressure force is increased potentially giving a higher ventilation rate through the space. This is the intention of designers when using a tall atrium connected to a naturally ventilated space. However, the atrium does not always enhance the flow in the space due to the extra constraint added by a_5 with effective area A_u $(m = 5, n = 5)$ to the effective area of the storey A_s. Adding A_u to A_s gives the total effective opening area A_t (with $m = 1$ and $n = 5$). Equating the volume flow rate through the ventilation system Q_s and the volume flow rate Q_h ($x = h$) in the plume at the interface height, Holford & Hunt [1] developed an expression relating the interface height and the geometrical parameters of the space and atrium:

$$\frac{A_t}{H^2} = \sqrt{C^3\xi^5/(M/H-\xi)} \quad (5)$$

From equation (5), the dimensionless interface height is only dependent on the dimensionless total effective opening area A_t/H^2 and the ratio of the atrium and the single space heights *M/H*. It is independent of the source strength B (*cf.* [5]).

When heat is added to the atrium above the storey level with a buoyancy flux of B_s (e.g. solar energy), the reduced gravity in the atrium g'_a is larger than g', and the stack pressure $\rho_o g'(H-h) + \rho_o g'_a(M-H)$ is larger than $\rho_o g'(M-h)$ (when the atrium is not heated). Therefore the presence of B_s provides another means of enhancing the ventilation flow rate through the space. This effect is equivalent to an increased atrium height. Replacing the original atrium height M with the increased atrium height M_{eff} equation (5) becomes:

$$\frac{A_t}{H^2} = \sqrt{C^3\xi^5/(M_{eff}/H-\xi)} \quad (6)$$

and it can be shown that $M_{eff} = M + B_s(M-H)/B$ [1]. In this case, the interface height is dependent on the ratio of the two buoyancy sources.

Small-scale laboratory experiments were conducted to validate the theoretical prediction (5) [1]. The salt-bath experimental technique uses Perspex models of a building, and brine introduced to fresh water to represent the effects of heat in air. Fresh water is used to represent ambient air. The model is then inverted and the flows visualised using dye or a shadowgraph. After correction for the virtual origin of the saline plume, which typically lies behind the actual origin [6], the dimensions of the experimental box with the tall atrium used by [1] were H =15.8cm and M =37.2cm, which lead to a ratio of M/H = 2.35. A TDC was used in the experiments channel the fresh water into the space from the external fresh water environment.

3 CFD modelling techniques

The CFD model in this work (Figure 2) uses air as the working fluid and its dimensions are ten times

greater than those used in the salt-bath experiments. In practice the flow inside the connected spaces is mixed by conduction, convection and radiation effects. In this work, conduction and radiation effects were neglected to meet the assumptions of the mathematical models and the experiments. The temperature difference between the upper and lower layers observed in the CFD simulations were greater than or equal to 2K. This corresponds to a Rayleigh number of the order of 1×10^{10}. It is therefore reasonable to consider the flow as fully turbulent although in some regions, e.g. near walls but away from the ventilation openings, the airflow could be laminar or weakly turbulent.

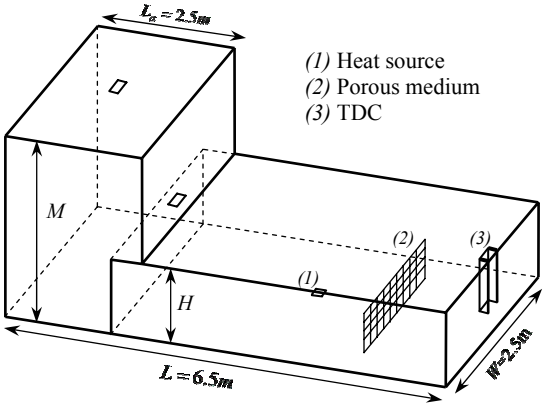

Figure 2. Geometry of CFD model

3.1 Numerical methods

It has been found [7] that two equation eddy-viscosity models are generally suitable for modelling indoor air flows, particularly when the enclosure is not heavily occupied and the first order fluid parameters are of the main interests (e.g. mean temperature, flow rate etc.) rather than turbulent fluctuation details. Previous studies suggested that the Renormalisation Group (RNG) k-epsilon model [8] performed better than other eddy-viscosity models in the prediction of indoor airflow features [3, 9]. In this work, the RNG k-epsilon model with a Boussinesq approximation was used. The full details of the governing equations for mass, momentum, thermal energy and the turbulence quantities can be found in [8].

The numerical investigation in this paper was carried out using CFX4, version 4.4 (2001) [10]. A Cartesian coordinate system with a structured mesh system was used and the hydrodynamic equation set solved in a segregated manner. The central differencing scheme was used to discretize the mass conservation equation; the momentum equations were discretized using the QUICK scheme; for all other equations, the hybrid scheme was used. Pressure coupling is treated using the SIMPLEC algorithms and the Rhie-Chow interpolation technique [11] is used to overcome the problem of decoupling due to co-located meshes.

Numerical studies of buoyancy-driven airflows are often subject to convergence difficulties due to the weak force driving the airflow. In this study false timesteps of 0.025s were used to further under-relax the momentum equations in order to achieve steady state solutions. False timesteps provide a means of tailoring the under-relaxation to the type of flow being considered. Convergence was considered to have been reached when the enthalpy residual was less than 1% of the total energy entering the domain and all other residuals varied by no more than 0.1% over the last 100 iterations.

3.2 Boundary conditions

The heat source was modelled as a no-slip wall boundary condition with a constant heat flux. A symmetry boundary bisecting all the ventilation openings and the heat source was used to reduce computing time. All other boundaries of the domain, except the ventilation openings, were modelled as no-slip wall boundaries with zero heat flux.

A constant pressure of 0 Pa (relative pressure) was imposed across the TDC inlet and the atrium outlet. However, this type of boundary at the ventilation openings in CFD does not represent the true physical nature of the flow due to loss coefficients either by expansion or discharge. Modelling some of the exterior airflow and moving the pressure boundary condition to the domain boundary overcome this but has the disadvantage of increasing the computational time and makes it difficult to determine the loss coefficient at the opening. In this work, the loss coefficients along the airflow path (at locations 1 to 5 in Figure 1) were treated in the following way.

By using a constant pressure boundary in CFX, the whole opening area becomes the effective area, therefore unity was assigned to C_{d1} and C_{d5} in equation (1). The friction loss coefficient along the TDC is given by $C_{d2} = D/4Lf$, where D and L are the diameter and length of TDC and $f \approx 5\times10^{-3}$ is the friction factor [12]. For cases considered in this work, $C_{d2} \geq 8.8$. This has less than 2% effect on the calculation of effective area A_n and was therefore ignored in equation (1). Airflow leaving the TDC experiences a sudden expansion; the cross section of the TDC is much smaller than the cross section of the single space therefore $C_{d3} \approx 1$ (page 119 of [13]). The storey outlet is a free opening within the airflow system which experiences loses due to contraction and expansion. For simplicity, a value of 0.63 was assumed here. In practice, the losses are density dependent [14, 15] and may vary significantly from this value. [1] examined the spread in their predictions due to this variation.

In order to maintain an upright plume a porous medium boundary was applied midway between the

TDC and the heat source (Figure 2). This prevented the horizontal inflow from impinging directly on the plume. In practice, ventilation systems are usually designed to minimise draughts, so the indoor airflow in natural ventilation system is commonly dominated by rising buoyant plumes.

3.3 Simulation conditions

Three sets of steady-state simulations were carried out as follow. In all cases, the ambient temperature was 15 ºC and the buoyancy flux B was 2.75×10^{-3} m^4s^{-3}.

(i) M/H = 2.35 was fixed, while the dimensionless total effective opening area was varied: A_t/H^2 = $(0.6, 0.8, 1.12, 1.60, 2.25, 3.05, 3.95, 4.75)\times10^{-2}$;

(ii) A_s/H^2 = 0.0177 and M/H = 2.35 were fixed, while the atrium outlet opening a_5 was varied giving A_u/H^2 = $(0.6, 1.2, 2.24, 2.69, 3.79)\times10^{-2}$;

(iii) A_t/H^2 = 0.008 was fixed, while M/H = (1.5, 2.35, 4.0, 5.0, 7.0).

For the last set of simulations, a buoyancy source B_s in the upper atrium can lead to the same effect as a taller atria, for example, M/H = (4.0, 5.0 and 7.0) is equivalent to M/H = 3.5 with B_s = (3.36, 5.40 and 9.47) $\times10^{-3}$ m^4s^{-3} (equation (6)).

4 Results and discussions

It took about 4000 iterations for the cases studied here with a mesh size of approximately 1.7×10^5 cells to achieve the convergence criteria.

Quantitative comparisons of non-dimensional interface heights, volume flow rates and temperature difference across the interface (represented by the reduced gravity g') are shown in Figures 3-7. Analytical and CFD results are shown in each figure. Experimental data [1] is available for the predictions of interface height and reduced gravity in the first set of simulations.

The interface heights predicted by the CFD model agreed well with those of the experimental and analytical work for values of A_t/H^2 less than 0.02 (equivalent to $\xi \approx 0.7$, see Figure 3a). For larger values of A_t/H^2 the interface height is under-predicted. In the CFD simulations, a layer of warm air remained beneath the ceiling for all values of A_t whereas the theory predicted 'complete ventilation' (e.g. ξ =1 for A_t/H^2 =0.0475). Experimental predictions showed the same trend. This discrepancy is thought to be caused by the assumption of a stationary fluid in the hydrostatic buoyant layer in the analytical model for all interface heights. In both experiments and CFD simulations, as the stratification level rises and the interface approaches the ceiling, the buoyant layer becomes unsteady and the homogeneous layer breaks down. The dimensionless volume flow rates through the system, Q_s/Q_H (where $Q_H = CB^{1/3}H^{5/3}$), predicted by the CFD model agree favourably with the analytical model even beyond A_t/H^2 =0.02. This is because the value of Q_s predicted by the CFD model (and the theory) depends on the size of the ventilation openings and the strength of the heat source but is not influenced by the position of the interface. Agreement is also good for the reduced gravity (Figure 3b).

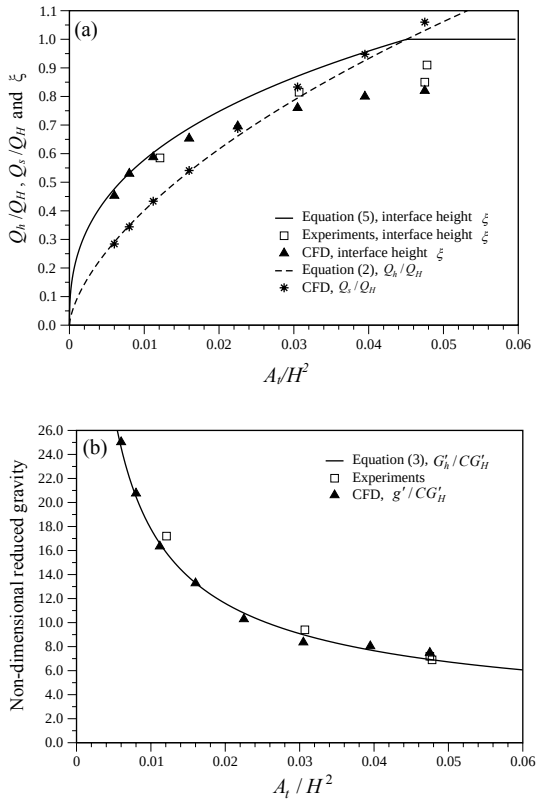

Figure 3. Variation of total effective area with (a) non-dimensional interface height and volume flow rate and (b) non-dimensional reduced gravity.

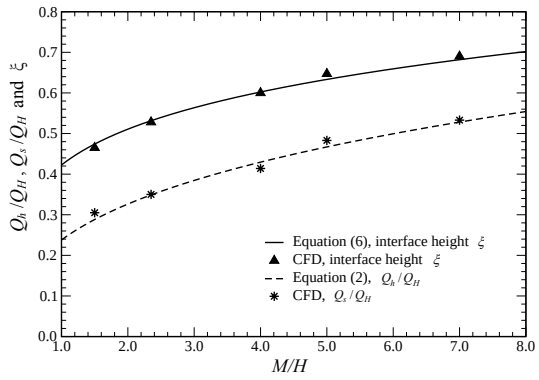

Figure 4. Variation of *M/H* with non-dimensional interface height and volume flow rates, for A_t/H^2 = 0.008.

Both interface heights and volume flow rates predicted by the CFD model for varying the stack heights and atrium outlet openings agreed favourably with the theory (Figures 4 & 5). In Figure 4, varying the ratio of *M/H* provides two methods of testing the CFD model. Firstly, the effect of physically increasing the atrium heights of the CFD model and secondly, the effect of adding buoyancy sources in an atrium of fixed height. CFD results in Figure 4 show the effect of increasing the atrium heights. Further work is underway in which heat input into the atrium is modelled explicitly to verify the theoretical model (Equation (6)). The two horizontal dashed lines (Figure 5) show the interface height and volume flow rate predicted by equations (4) and (2) for the single space with A_s/H^2 =0.0177. Below the two lines the constraint added by the atrium opening overcomes the enhancement of the flow induced by a tall atrium. Therefore both the flow rates and interface heights are lower than the single storey without an atrium. Above the two lines, the atrium enhances the flow rate because the size of the atrium outlet increases.

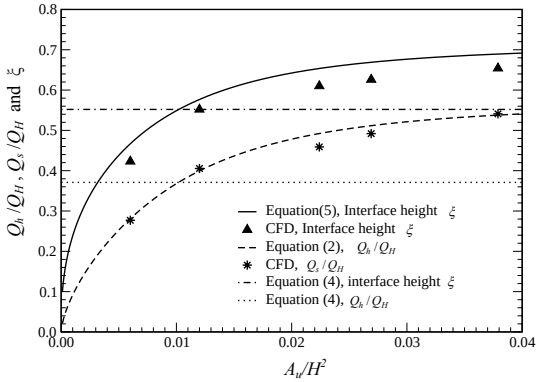

Figure 5. Variation of interface height and volume flow rate with A_t/H^2 (for A_s/H^2 =0.0177, and *M/H*=2.35).

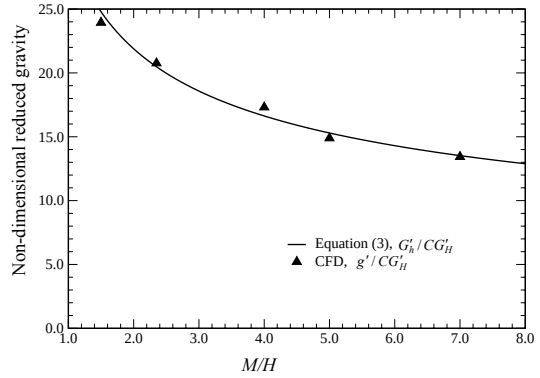

Figure 6. Variation of non-dimensional reduced gravity with *M/H*, for A_t/H^2 = 0.008

Good agreement was also achieved for the predictions of the reduced gravities for the second and third sets of simulations (Figures 6 & 7). This is because the interface heights remained below 0.7 for the cases considered. Within this range CFD performed better in the predictions of interface height (Figures 4 & 5), which is also shown in Figure 3.

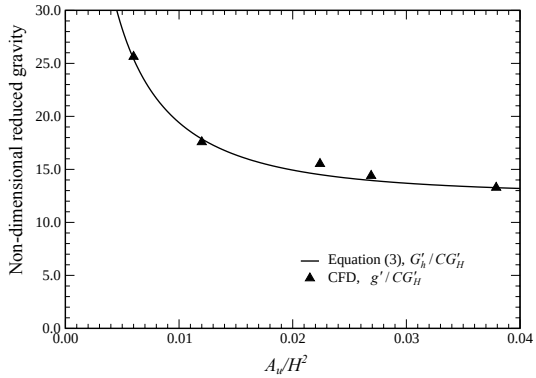

Figure 7. Variation of non-dimensional reduced gravity with A_t/H^2, for A_s/H^2 =0.0177, and *M/H*=2.35

Qualitative comparison between the experiments and CFD showed good agreement for the air flow pattern in the space but not in the atrium (Figure 8). For the salt-bath experiments [1], a density interface exists in the atrium at the outlet level of the storey separating an ambient, stagnant layer from a warm, buoyant layer above-suggesting that the warm air leaving the storey does not mix with the ambient layer below. However, in the CFD predictions the atrium air is fully mixed (Figure 8). This is caused by the diffusion terms in the energy and turbulence equations and the steady-state nature of the CFD simulations which assume that the flow evolves over an infinite period of time. Even when the diffusion terms in CFD equations were manually reduced, the CFD model still predicted a well mixed atrium in the steady state.

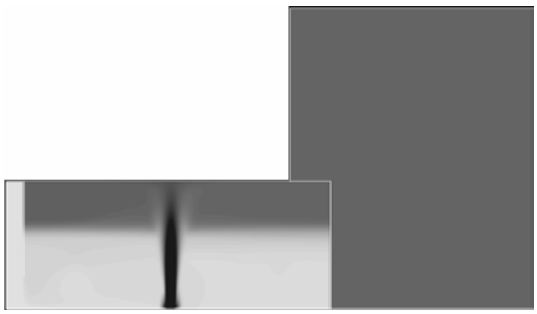

Figure 8. CFD prediction showing the temperature distribution in the single storey and the atrium (darker regions denote warmer air)

When a transient simulation was run, an interface in the atrium was observed but this was unsteady and gradually descended, again resulting in a well-mixed atrium after about 13.5 hours of real time. Diffusivity of brine in water is much smaller than the diffusivity of heat in air, therefore it is possible that, if the experiments were run for a longer period of time, the atrium would eventually become well mixed.

5 Conclusions

Steady-state simulations of natural ventilation flows in a single storey space connected to a tall atrium have been undertaken. The numerical results showed the ability of CFD for modelling natural displacement ventilation flows driven by thermal buoyant plumes in connected spaces. Favourable agreement was achieved between the mathematical models, experiments and CFD for the predictions of the non-dimensional volume flow rates and reduced gravities. For the predictions of interface height, quantitative discrepancies were observed. This is thought to be due to the assumption in the analytical model that the buoyant layer remains homogenous and hydrostatic for all interface heights which was not the case in the CFD and experimental work as the interface approached the ceiling. A qualitative discrepancy was observed in the atrium space whereby the CFD model did not predict the stagnant layer at the base of the atrium observed in the experiments. One possible reason for this could be the low diffusivity of brine in water relative to heat in air, resulting in reduced diffusion and a slower descent of the interface in the atrium.

A constant pressure boundary was imposed directly at the ventilation openings. Therefore the reduction in opening area due to discharge and expansion effects was neglected. Hence, the loss coefficients at these locations are equal to unity. As a consequence, the physical opening sizes for the CFD simulation are smaller than those used in the theory and experiments although the effective opening areas were the same. Using this method, it is no longer necessary to explicitly model airflow outside the connected boxes to take into account the effect of the loss coefficients. Hence, this method potentially reduces the computational cost and avoids the uncertainties of modelling the loss coefficients. The close agreement of the CFD predictions with the analytical and experimental work suggests that the CFD performed well in predicting the effects of the contraction at the storey outlet opening, and that the application of constant pressure boundary with unity loss coefficient is robust.

It was found that a porous medium boundary was necessary to maintain a vertically rising thermal plume as assumed in the theory.

References

[1] J. M. Holford and G. R. Hunt. Fundamental atrium design for natural ventilation. *Building and Environment,* 38, 409-426, 2003.

[2]. J. G. Symons and M. K. Peck. Natural convection heat transfer through inclined longitudinal slots, *J Heat Transfer*, 106, 824-829, 1984.

[3]. M. J. Cook and K. J. Lomas. Buoyancy-driven displacement ventilation flows: Evaluation of two eddy viscosity models for prediction. *Building Services Engineering Research and Technology,* 19, No. 1, 15-21, 1998.

[4] B. R. Morton, G. I. Taylor & J. S. Turner. Turbulent gravitational convection from maintained and instantaneous sources. *Proc. Roy. Soc*. A 234. 1-23, 1956.

[5] P. F. Linden, G. Lane-Serff and D. A. Smeed. Emptying filling boxes: the fluid mechanics of natural ventilation. *J. Fluid Mech.,* Vol. 212 pp. 309-335, 1990.

[6] G. R. Hunt and N. G. Kaye. Virtual origin correction for lazy turbulent plumes. *J. Fluid Mech.*, 435, pp.377-396, 2001.

[7] Q. Chen. Comparison of different k- models for indoor air flow computations. *Numerical Heat Transfer, Part B*, 28; pp. 353-369, 1995.

[8] V. Yakhot, S. A. Orszag, S. Thangham, T. B. Gatski and C. G. Speziale. Development of turbulence models for shear flows by a double expansion technique. *Phys. Fluids A*, 4(7), pp. 1510-1520, 1992.

[9] G. Gan. Prediction of turbulent buoyant flow using an RNG k-ε model. *Numerical Heat Transfer, Part A*, 33; pp. 169-189, 1998.

[10] CFX. User Guide Version 4.4. *CFX International*, Harwell, UK, 2001.

[11] C. M. Rhie and W. L. Chow. Numerical study of the turbulent flow past an airfoil with trailing edge separation. *American Inst. Aeronautics and Astronautics J*. 21 (11), pp. 1527-1532, 1983.

[12] G. R. Hunt and J. M. Holford. Top-down natural ventilation of multi-story buildings. *19th Annual AIVC conference, Oslo, Norway*, pp. 197-205, September 1998.

[13] Y. Nakayama & R. F. Boucher. An introduction of fluid mechanics. ISBN 0340 67649 3, 1999.

[14] G.R. Hunt & J.M. Holford. The discharge coefficient - experimental measurement of a dependence on density contrast. *Proc. 21st AIVC Conf.*, The Hague, Netherlands. 12pp. 2000.

[15] J.M. Holford & G.R. Hunt. The dependence of the discharge coefficient on density contrast - experimental measurements. *Proc. 14th Australasian Fluid Mechanics Conf.* 9-14th December 2001, Adelaide University, Adelaide, NSW, Australia, 1, 123-126. Editor B.B.Dally, ISBN 1 876346 34 5 2001.